Inorganic Chemistry

Article

pubs.acs.org/IC

Photoinduced Water Oxidation by a Tetraruthenium Polyoxometalate Catalyst: Ion-pairing and Primary Processes with $Ru(bpy)_3^{2+}$ Photosensitizer

Mirco Natali,[†] Michele Orlandi,[†] Serena Berardi,[§] Sebastiano Campagna,*[,‡] Marcella Bonchio,[§] Andrea Sartorel,*[,§] and Franco Scandola*[,†]

[†]Dipartimento di Chimica and Centro Interuniversitario per la Conversione Chimica dell'Energia Solare (SOLARCHEM), sezione di Ferrara, via Borsari 46, 44121 Ferrara, Italy

[‡]Dipartimento di Chimica Inorganica, Chimica Analitica e Chimica Fisica, Università di Messina and Centro Interuniversitario per la Conversione Chimica dell'Energia Solare (SOLARCHEM), sezione di Messina, Via Sperone 31, 98166 Messina, Italy

[§]ITM-CNR and Department of Chemical Sciences, University of Padova, Via Marzolo, 1, 35131 Padova, Italy

Supporting Information

ABSTRACT: The tetraruthenium polyoxometalate $[Ru_4(\mu\text{-}O)_4(\mu\text{-}OH)_2(H_2O)_4(\gamma\text{-}SiW_{10}O_{36})_2]^{10-}$ (**1**) behaves as a very efficient water oxidation catalyst in photocatalytic cycles using $Ru(bpy)_3^{2+}$ as sensitizer and persulfate as sacrificial oxidant. Two interrelated issues relevant to this behavior have been examined in detail: (i) the effects of ion pairing between the polyanionic catalyst and the cationic $Ru(bpy)_3^{2+}$ sensitizer, and (ii) the kinetics of hole transfer from the oxidized sensitizer to the catalyst. Complementary charge interactions in aqueous solution leads to an efficient static quenching of the $Ru(bpy)_3^{2+}$ excited state. The quenching takes place in ion-paired species with an average **1**:$Ru(bpy)_3^{2+}$ stoichiometry of 1:4. It occurs by very fast (ca. 2 ps) electron transfer from the excited photosensitizer to the catalyst followed by fast (15−150 ps) charge recombination (reversible oxidative quenching mechanism). This process competes appreciably with the primary photoreaction of the excited sensitizer with the sacrificial oxidant, even in high ionic strength media. The $Ru(bpy)_3^{3+}$ generated by photoreaction of the excited sensitizer with the sacrificial oxidant undergoes primary bimolecular hole scavenging by **1** at a remarkably high rate ($3.6 \pm 0.1 \times 10^9$ M^{-1} s^{-1}), emphasizing the kinetic advantages of this molecular species over, e.g., colloidal oxide particles as water oxidation catalysts. The kinetics of the subsequent steps and final oxygen evolution process involved in the full photocatalytic cycle are not known in detail. An indirect indication that all these processes are relatively fast, however, is provided by the flash photolysis experiments, where a single molecule of **1** is shown to undergo, in 40 ms, ca. 45 turnovers in $Ru(bpy)_3^{3+}$ reduction. With the assumption that one molecule of oxygen released after four hole-scavenging events, this translates into a very high average turnover frequency (280 s^{-1}) for oxygen production.

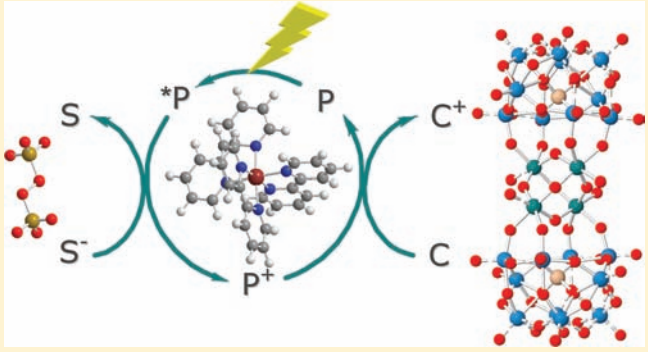

INTRODUCTION

Oxidation of water to molecular oxygen is a key step common to most artificial photosynthetic reaction schemes.[1] It is a very complex process, involving the four-electron oxidation of two water molecules, the formation of a new O−O bond, and the release of four protons. As such, water oxidation is considered to be the real kinetic bottleneck toward artificial photosynthesis.[2] In recent years, substantial progress has been made in the development of catalysts for oxygen evolution, both as heterogeneous (colloidal metal oxides,[3−6] electrodeposited films[7]) and homogeneous (mono-[8,9] and polynuclear[10−13] metal complexes) systems.

A number of tetrametallic molecular catalysts, bearing structural (and possibly also functional) affinity to the oxygen evolving center (OEC) of photosystem II,[14] have recently been reported.[15−19] By virtue of their robustness when exposed to the harsh conditions of oxygen evolution catalysis, all-inorganic polyoxometalates (POMs) embedding a multiredox tetrametallic core are receiving great attention. Two such systems, $[Ru_4(\mu\text{-}O)_4(\mu\text{-}OH)_2(H_2O)_4(\gamma\text{-}SiW_{10}O_{36})_2]^{10-}$ (**1**, see Figure 1)[15,16] and $[Co_4(H_2O)_2(PW_9O_{34})_2]^{10-}$,[18,20] have been synthesized and used in homogeneous water oxidation with strong chemical oxidants (dark cycles)[15a,16a,18a] or in photocatalytic cycles employing sacrificial electron acceptors.[16b,18b,21] In the case of the tetra-cobalt species $[Co_4(H_2O)_2(PW_9O_{34})_2]^{10-}$, however, serious doubt has been cast on the molecular nature of the catalyst. In fact, in electrochemical water oxidation the

Received: April 5, 2012
Published: June 11, 2012

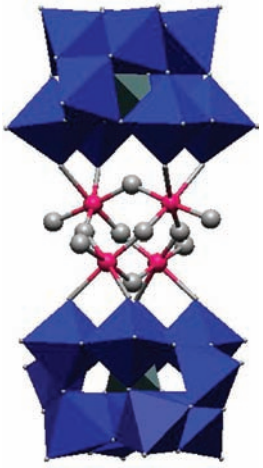

Figure 1. Structure of the tetrametallic catalyst $[Ru_4(\mu\text{-}O)_4(\mu\text{-}OH)_2(H_2O)_4(\gamma\text{-}SiW_{10}O_{36})_2]^{10-}$[15,16] emphasizing the Ru_4–oxo–hydroxo core.

actual catalytic species has been shown[22] to be heterogeneous cobalt oxide, generated following dissociation of the original molecular precursor.[23,24] Catalyst **1**, on the other hand, with the more inert ruthenium cluster, has been shown to be stable in water oxidation under turnover conditions.[15a,16c] Furthermore, no evidence of catalyst instability has been observed in the time-resolved experiments described below, which have been found to give identical results using freshly prepared (experiment performed within 1 min after dissolution) or aged (up to 3 h) solutions of **1**.

In a standard photocatalytic cycle (Figure 2), a strong oxidant (P^+) is irreversibly generated by reaction of an excited

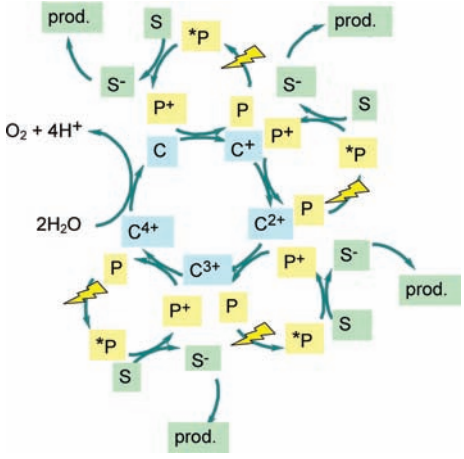

Figure 2. Sequential electron transfer mechanism for oxygen evolution in a sacrificial cycle involving a photosensitizer (P), a sacrificial electron acceptor (S), and a tetrametallic catalyst (C). C^{n+} (n = 1–4) denotes the four sequentially oxidized forms of the catalyst, regardless of the actual charge type of the catalyst. Products of irreversible reduction of the sacrificial acceptor indicated as "prod.".

photosensitizer (P) and a sacrificial electron acceptor (S) that decomposes upon reduction, shutting down any reversible phenomena and being the limiting reagent for product yield.

The photocatalytic mechanism leading to water oxidation is generally assumed to involve four sequential hole transfer steps from the photochemically oxidized sensitizer to the catalyst, which then evolves to a series of high valent intermediates. In the experimental oxygen evolution studies, relevant practical parameters, such as chemical and quantum yields, turnover numbers (TONs), and turnover frequencies (TOFs), have been determined to evaluate the overall system performance. Very rarely, however, time-resolved techniques have been applied to the detection of elementary processes and transient intermediates.[6b,25]

Time-resolved techniques can provide kinetic information of great importance for the optimization of oxygen-evolving sacrificial cycles and, in perspective, of photochemical water splitting systems. In principle, the rates of hole transfer from the oxidized sensitizer (S^+) to the catalyst along its evolution pathway (C, C^+, ...,C^{4+}) can be measured by appropriate laser flash photolysis experiments. In sacrificial cycles, as represented in Figure 2, the oxidized sensitizer is irreversibly produced so that, in principle, very fast hole transfer is not a strict requirement. In practice, however, the sensitizers, in their oxidized form, are often unstable under the reaction conditions used,[6a,26] and fast hole scavenging is pivotal to minimize their decomposition (usually the main limiting factor in terms of turnover performance). On the other hand, fast hole-transfer rates will become absolutely crucial in regenerative systems where the catalyst must be able to scavenge the hole on the photogenerated oxidant in competition with charge recombination. Kinetic studies of this type have been used, for instance, by Mallouk to optimize the performance of colloidal IrO_2 as a water oxidation catalyst,[6b] prior to its inclusion in a dye-sensitized photoelectrochemical cell for photoassisted water splitting.[6d]

We report herein a detailed study addressing the kinetics of hole transfer processes involved in sacrificial systems as depicted in Figure 2, where the sensitizer P is $Ru(bpy)_3^{2+}$, the sacrificial acceptor S is $S_2O_8^{2-}$, the decomposition products of S^- are SO_4^{2-} and $SO_4^{\bullet-}$,[27−29] and the tetraruthenium POM **1** is used as the catalyst C.[30] Given the high negative charge of the catalyst, special attention has been paid to ion pairing association of **1** with the cationic sensitizer and its photophysical and kinetic consequences.

EXPERIMENTAL SECTION

Materials. For photophysical measurements Milli-Q Ultrapure water and related buffer solutions were used. Other chemicals were all of reagent grade quality.

Syntheses. Catalyst **1** was synthesized following literature procedures.[15a] A 262 mg (0.36 mmol) portion of $K_4Ru_2OCl_{10}$ was dissolved in 30 mL of deionized water; 1 g (0.34 mmol) of $K_8\gamma\text{-}SiW_{10}O_{36}\cdot 12H_2O$ was then added. $(NH_4)_2RuCl_6$ can be used as an alternative ruthenium precursor, instead of $K_4Ru_2OCl_{10}$. The dark-brown solution is kept at 70 °C for 1 h, and then allowed to cool at room temperature and filtered. Excess of CsCl (4.4 g) is added to precipitate **1** as the cesium salt. This latter is transformed into the sodium salt by ion-exchange chromatography; the crude sodium salt is then purified by exclusion dimensional chromatography, with total yield = 80%.

Apparatus and Procedures. UV–vis spectra were recorded with a UV–vis–NIR Jasco V-570 spectrophotometer. Luminescence spectra were taken on a Spex Fluoromax-2 equipped with Hamamatsu R928 tubes.

Femtosecond time-resolved experiments were performed using a pump–probe setup[31] based on the Spectra-Physics Hurricane Ti:sapphire laser source and the Ultrafast Systems Helios spectrometer. The 400-nm pump pulses were generated with a Spectra Physics SHG. Probe pulses were obtained by continuum generation on a sapphire plate (useful spectral range: 450–800 nm). Effective time

dx.doi.org/10.1021/ic300703f | Inorg. Chem. 2012, 51, 7324–7331

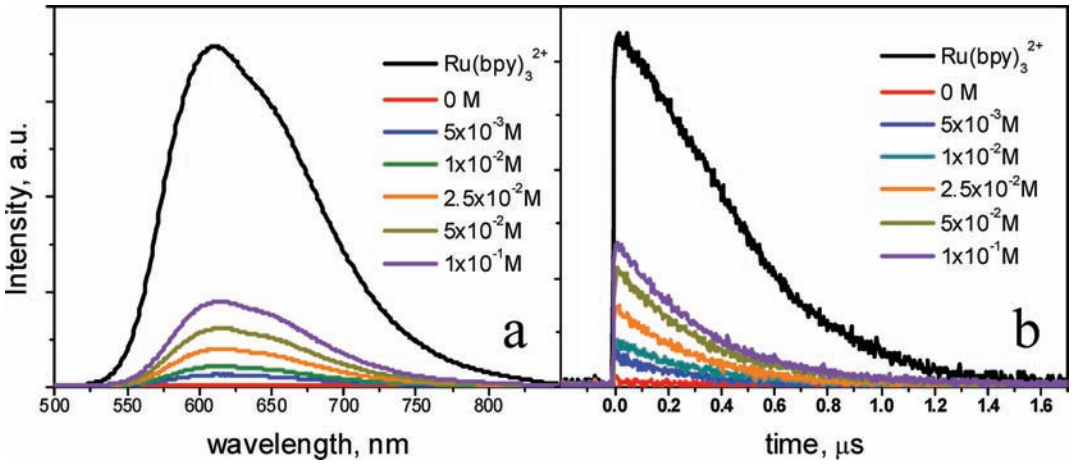

Figure 3. "Dequenching" of the $Ru(bpy)_3^{2+}$ emission upon addition of Na_2SO_4 to an aqueous solution containing 5.0×10^{-5} M $Ru(bpy)_3^{2+}$ and 5.0×10^{-5} M **1**. Results of stationary (a, excitation at 450 nm) and pulsed (b, excitation at 355 nm) experiments. Data corrected for the inner filter effect of **1** at the excitation wavelength. The black curves refer to 5.0×10^{-5} M $Ru(bpy)_3^{2+}$ (neither catalyst nor salt added).

resolution is ca. 300 fs, temporal chirp over the white-light 450−750 nm range is ca. 200 fs, and temporal window of the optical delay stage is 0−2000 ps. The time-resolved spectral data were analyzed with the Ultrafast Systems Surface Explorer Pro software.

Nanosecond transient absorption measurements were performed with an Applied Photophysics laser flash photolysis apparatus, using a frequency-doubled (532 nm, 330 mJ) or tripled (355 nm, 160 mJ) Surelite Continuum II Nd/YAG laser (half-width 6−8 ns) as excitation source. Transient detection was obtained in the kinetic mode using a photomultiplier−oscilloscope combination (Hamamatsu R928, LeCroy 9360) or in the spectroscopic mode with a Princeton Instruments gated intensified CCD-Camera PI-MAX II equipped with an Acton SpectraPro 2300i triple grating flat field monochromator, an RB GenII intensifier, an ST133 controller, and a PTG pulser. The probe light was filtered through bandpass filters: centered at 450 nm (fwhm 10 nm) in the kinetic mode, centered at 500 nm (fwhm 200 nm) in the spectroscopic mode.

RESULTS AND DISCUSSION

The electrochemistry of catalyst **1** in aqueous acidic solutions shows several equally spaced (ca. 0.2 V) redox processes in the −0.5/1.0 V versus SCE range.[15b,16c] The catalyst, which as an alkaline salt has the tetraruthenium core in the diamagnetic (IV,IV,IV,IV) state, in aerated aqueous acidic solution is found to be present as a paramagnetic[15b] species, likely the (IV,IV,IV,V) singly oxidized form.[32] This is also true in the neutral solutions used in this work, as shown by an EPR signal with g_x, g_y, and g_z values of 1.97, 1.67, and 1.43, respectively (Figure S1 of Supporting Information).

In an aqueous solution containing 5.0×10^{-5} M $Ru(bpy)_3^{2+}$ and 5.0×10^{-5} M **1**, the emission of the sensitizer is completely quenched. The quenching process takes place within sensitizer−catalyst ion-paired species, as demonstrated by the "dequenching" effect of ionic strength: the $Ru(bpy)_3^{2+}$ emission builds up when Na_2SO_4 is added to the solution (Figure 3a). The constant lifetime of the growing emission (370 ns), coincident with that of free $Ru(bpy)_3^{2+}$ in aerated water solution (Figure 3b), demonstrates the static nature of the quenching process.

As to the nature of the ion-paired species, the presence in solution of **1**, $Ru(bpy)_3^{2+}$, and their counterions (Na^+ and Cl^-, respectively) will likely lead to a complex distribution of variously ion-paired species. Fluorescence titration of $Ru(bpy)_3^{2+}$ with **1** (Figure 4) and conductometric titration of **1** with $Ru(bpy)_3^{2+}$ (Figure 5) can be used to monitor this type of aggregation in aqueous solutions. Both measurements indicate the formation of aggregates with an average $[\mathbf{1}]/[Ru(bpy)_3^{2+}]$ ratio close to 1/4. This corresponds to the notion that, owing to its high negative charge (10−), a single **1** anion can bind multiple $Ru(bpy)_3^{2+}$ cations.

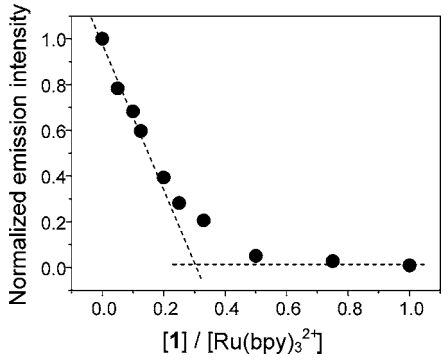

Figure 4. Fluorimetric titration of $Ru(bpy)_3^{2+}$ (5.0×10^{-5} M) with **1** in aqueous solution.

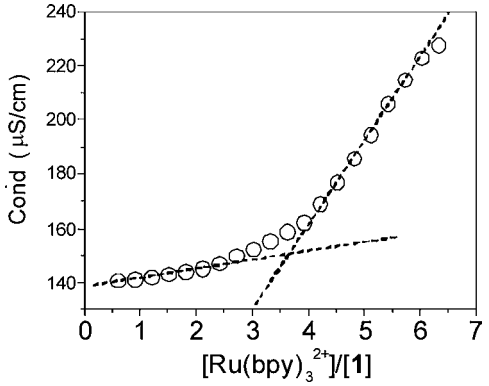

Figure 5. Conductometric titration of **1** (5.0×10^{-5} M) with $Ru(bpy)_3^{2+}$ in aqueous solution.

The quenching process taking place within the ion-paired species can be investigated in the subnanosecond time scale by ultrafast spectroscopy (Figure 6). The initial spectrum, with

dx.doi.org/10.1021/ic300703f | Inorg. Chem. 2012, 51, 7324−7331

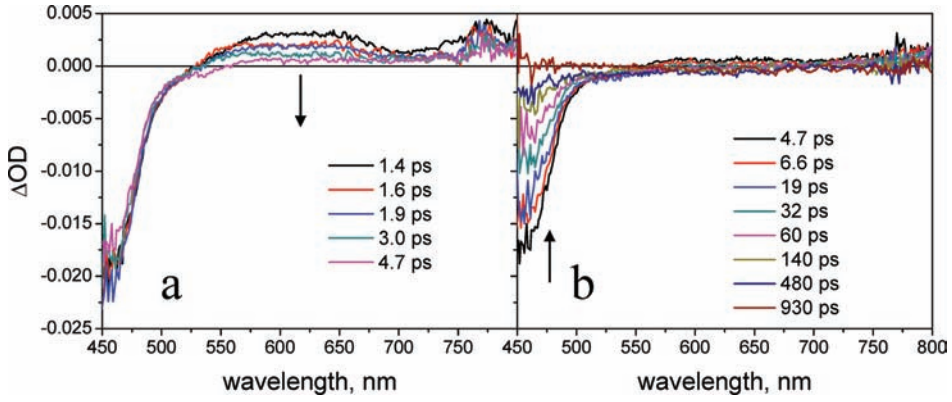

Figure 6. Ultrafast spectroscopy (excitation at 400 nm) of an aqueous solution containing 2.0×10^{-4} M $Ru(bpy)_3^{2+}$ and 2.0×10^{-4} M **1**. Biphasic behavior: qualitatively different spectral changes in the (a) 1.4−4.7 ps and (b) 4.7−930 ps time ranges.

bleaching of the ground-state MLCT band at 450 nm and weak, broad, positive absorption at $\lambda > 530$ nm, is the typical spectrum of the $Ru(bpy)_3^{2+}$ MLCT excited state.[33] The subsequent spectral changes are clearly biphasic. In the first few picoseconds, the positive absorption disappears while the bleach remains almost constant (Figure 6a). Then, the bleach disappears completely, decaying smoothly to the baseline (Figure 6b). The time constant of the first process is ca. 2 ps; the second decay has a complex kinetic, requiring at least two time constants (ca. 15 and 150 ps) for a reasonable fit. In terms of mechanisms, possible hypothesis are (i) an oxidative quenching (electron transfer from the excited sensitizer to **1**) or (ii) a reductive quenching (electron transfer from **1** to the excited sensitizer), in both cases followed by back electron transfer. In fact, the transient spectral changes of Figure 6 are quite typical for processes of the first type, with $Ru(bpy)_3^{3+}$ (MLCT band bleached, no additional absorption in this spectral range) being produced in the forward step.[34] The tetrametallic core in **1** has indeed several accessible reduction steps[15b,16c] to make oxidative quenching of the $Ru(bpy)_3^{2+}$ excited state energetically allowed.

The formation of ion pairs between $Ru(bpy)_3^{2+}$ and **1**, with ultrafast quenching of the sensitizer excited state, is relevant to the use of these units in sacrificial cycles such as that depicted in Figure 2, which require an efficient reaction of the excited sensitizer with the sacrificial acceptor. In fact, complications inherent to ion-pair formation clearly show up (see below) in laser flash photolysis experiments intended to measure rates of hole-transfer between the oxidized sensitizer and the catalyst. In these experiments, a given concentration of oxidized sensitizer is generated "instantaneously" (i.e., within 10 ns) by photoreaction of the sensitizer with the sacrificial acceptor, and its rereduction by the catalyst can be monitored in time over a relatively wide window (0−100 ms). The instantaneous formation of $Ru(bpy)_3^{3+}$ is detected as a general bleach of the metal-to-ligand charge transfer absorption of $Ru(bpy)_3^{2+}$, and its reduction by the catalyst can be monitored following the recovery of the bleach back to the initial baseline (Figure S2 of Supporting Information). In the experiment illustrated in Figure 7, aqueous solutions containing 5.0×10^{-5} M $Ru(bpy)_3^{2+}$, 5.0×10^{-3} M $Na_2S_2O_8$, and 8.0×10^{-2} M phosphate buffer at pH 7 are excited with 8-ns pulses of 355-nm light, and the disappearance of $Ru(bpy)_3^{3+}$ is monitored as a function of the concentration of **1** (varied in the range 0−5.0×10^{-5} M). The evident qualitative result is that $Ru(bpy)_3^{3+}$ (as monitored by the bleach at 450 nm) is reduced back to

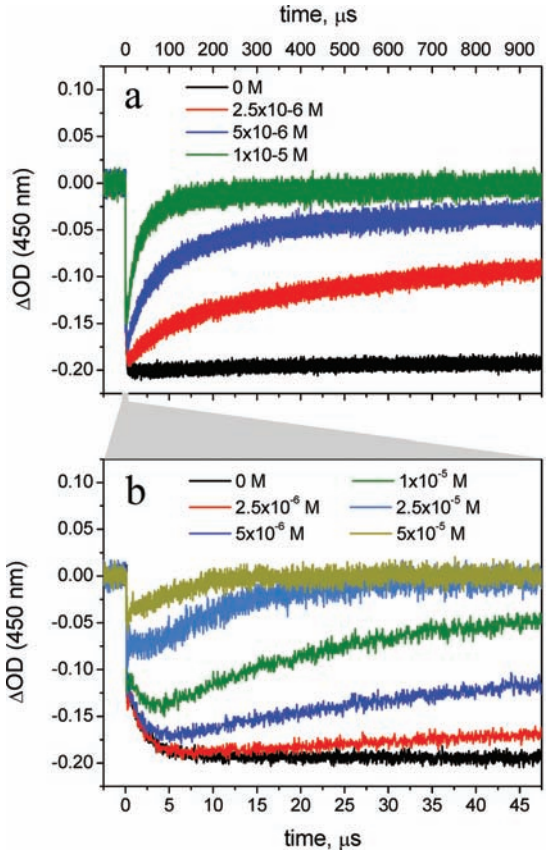

Figure 7. Flash photolysis of aqueous solutions containing 5.0×10^{-5} M $Ru(bpy)_3^{2+}$, 5.0×10^{-3} M $Na_2S_2O_4$, 8.0×10^{-2} M phosphate buffer (pH 7), and variable concentrations of **1** (0−5.0×10^{-5} M). Excitation with 8-ns pulses of 355-nm light. (a) Full time scale (0−1 ms). (b) Details of the early time scale (0−47 μs).

$Ru(bpy)_3^{2+}$ with kinetics dependent on the catalyst concentration. The hole-transfer rate constant can be easily obtained from the decays at high catalyst concentrations ($\geq 2.5 \times 10^{-5}$ M, traces shown in Figure 7b and omitted for clarity in Figure 7a) where the kinetics of recovery becomes pseudo-first-order (Figure S3 of Supporting Information). The high value obtained ($3.6 \pm 0.1 \times 10^9$ $M^{-1}s^{-1}$)[35] confirms that the molecular catalyst **1** is superior, in this respect, to some of the best colloidal catalysts, such as, e.g., IrO_x (for which values of the order of 10^6 M^{-1} s^{-1} have been measured).[6a] Some intriguing aspects are revealed by these results, however, when

dx.doi.org/10.1021/ic300703f | Inorg. Chem. 2012, 51, 7324−7331

Scheme 1

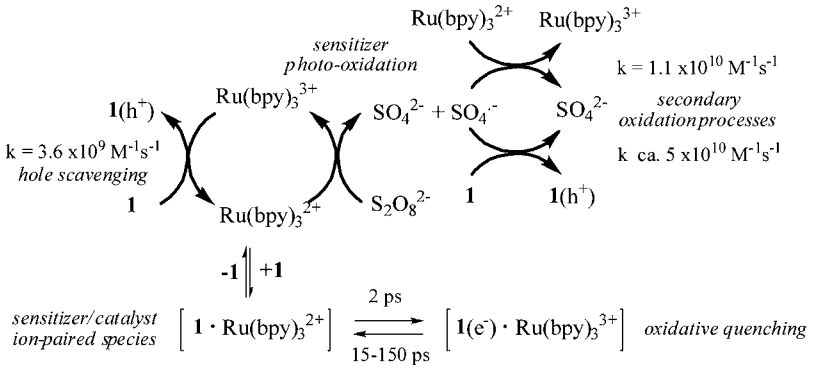

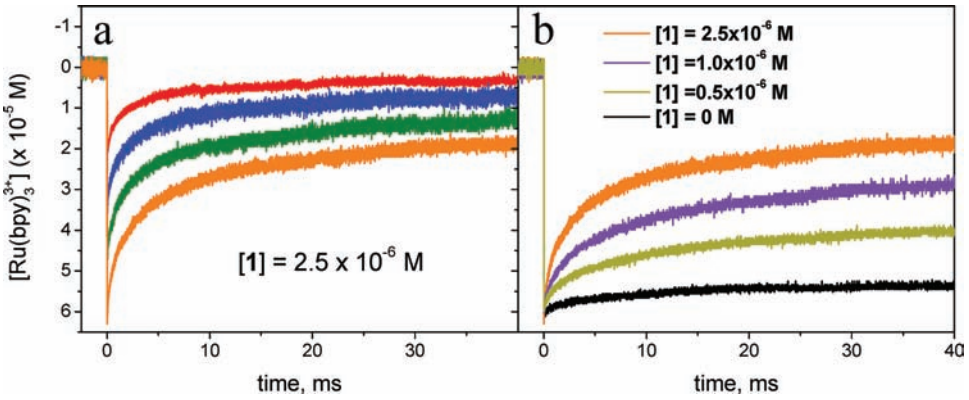

Figure 8. Reduction of photogenerated $Ru(bpy)_3^{3+}$ (from bleach recovery at 450 nm) by **1**. (a) [**1**] = 2.5 × 10^{-6} M, initial concentration of $Ru(bpy)_3^{3+}$ varied in the range 2.2−6.3 × 10^{-5} M with increasing laser power. (b) Initial [$Ru(bpy)_3^{3+}$] = 6.3 × 10^{-5} M, [**1**] varied in the range 2.5−0.5 × 10^{-6} M (black trace: control experiment at initial [$Ru(bpy)_3^{3+}$] = 6.3 × 10^{-5} M in the absence of **1**).

the early time scale of the experiment is magnified as in Figure 7b. In the absence of **1**, the formation of $Ru(bpy)_3^{3+}$ clearly exhibits a prompt and delayed component of almost equal amplitude, the former corresponding to the primary photoreaction between the excited $Ru(bpy)_3^{2+}$ and $S_2O_4^{2-}$ and the latter to the secondary dark reaction between the oxidizing SO_4^{-} radical ion and $Ru(bpy)_3^{2+}$.[28,36] The addition of the catalyst, besides speeding up the disappearance of $Ru(bpy)_3^{3+}$ in the long time scale (Figure 7a), also has pronounced effects on its formation (Figure 7b). In particular, as the concentration of **1** is increased, (i) the amount of $Ru(bpy)_3^{3+}$ formed promptly undergoes a strong decrease and (ii) the secondary process becomes less and less efficient (and practically disappears for [**1**] = 5 × 10^{-5} M). The reason for the first effect lies in the above-described ion pairing phenomenon (which, although less pronounced than in pure aqueous solution, is still effective at the relatively high ionic strength used in these experiments, see Figure 3): only the fraction of excited $Ru(bpy)_3^{2+}$ that is not ion-paired with (and thus instantaneously quenched by) **1** is able to generate $Ru(bpy)_3^{3+}$ by reaction with persulfate.[37] The second effect very likely reflects the fact that as the concentration of **1** increases, the SO_4^{-} radical ion produced in the primary process starts to oxidize **1** instead of $Ru(bpy)_3^{2+}$.[38]

The complex set of processes responsible for the observed behavior is summarized in Scheme 1.

Some interesting observations can be made when the data in Figure 7a are considered from a quantitative viewpoint. The concentration of photochemically generated $Ru(bpy)_3^{3+}$ in Figure 7, as obtained from the initial absorbance change,[39] is in the range 2.0−1.4 × 10^{-5} M (depending on the catalyst concentration for the above-mentioned ion-pair quenching effects). The interesting point is that, at low catalyst concentrations, the amount of $Ru(bpy)_3^{3+}$ being reduced within the time window of the laser flash photolysis experiment can largely exceed the amount of catalyst present in solution. For instance (red and blue curves in Figure 7a), 2.5 × 10^{-6} M **1** is able to reduce 1.0 × 10^{-5} M $Ru(bpy)_3^{3+}$, and 5.0 × 10^{-6} M **1** consumes 1.4 × 10^{-5} M $Ru(bpy)_3^{3+}$. This clearly means that in the time window of the laser flash photolysis experiment a single catalyst molecule undergoes several (ca. 4) consecutive hole transfer steps which amounts to saying that in these conditions the whole 4-h^+ charging sequence of the catalyst (Figure 2) takes about one millisecond. Thus, depending on the ratio between oxidized sensitizer and catalyst, the flash photolysis experiments are suited not only to measure rates of hole transfer (using excess catalyst) but also to observe the process under true catalytic conditions (having excess oxidized sensitizer). So it is possible to proceed further into the catalytic domain by pushing up the initial concentration of $Ru(bpy)_3^{3+}$ (using 1.0 × 10^{-4} M $Ru(bpy)_3^{2+}$ solution and increasing laser power, Figure 8a) or by further lowering the concentration of **1** (Figure 8b).

Figure 8a shows clearly that in the catalytic regime the kinetics of $Ru(bpy)_3^{3+}$ reduction is largely independent of the initial concentration of the oxidized sensitizer in the 2.2−6.3 × 10^{-5} M range (ca. 70% is always reduced by 2.5 × 10^{-6} M **1** within the time window of the experiment). Figure 8b, on the other hand, shows rather impressive results in terms of turnover (TON). For instance, in 40 ms, 2.5 × 10^{-6} M **1** reduces ca. 4.4

dx.doi.org/10.1021/ic300703f | Inorg. Chem. 2012, 51, 7324−7331

$\times 10^{-5}$ M $Ru(bpy)_3^{3+}$, meaning that ca. 18 holes are transferred per catalyst molecule. This means that not only the whole charging sequence, but also the discharge of the C^{4+} catalyst by water oxidation (Figure 2), takes place efficiently within this time scale, with ca. 4.4 full catalytic oxygen evolving cycles being accomplished by **1** in 40 ms following the laser flash. As the catalyst concentrations are lowered (Figure 8b), the TONs for oxygen evolution (defined as $^1/_4\ \Delta[Ru(bpy)_3^{3+}]/[\mathbf{1}]$) obtained in 40 ms increase as follows: $[\mathbf{1}] = 2.5 \times 10^{-6}$ M, $TON_{(40\ ms)} = 4.4$; $[\mathbf{1}] = 1.0 \times 10^{-6}$ M, $TON_{(40\ ms)} = 8.6$; $[\mathbf{1}] = 0.5 \times 10^{-6}$ M, $TON_{(40\ ms)} = 11.2$. These numbers translate into very high values of average turnover frequency for oxygen formation, defined as $TOF_{av} = (^1/_4\Delta[Ru(bpy)_3^{3+}]/\Delta t)/[\mathbf{1}]$. For instance, with $[\mathbf{1}] = 0.5 \times 10^{-6}$ M, the TON obtained over 40 ms corresponds to the rather spectacular TOF_{av} value of 280 s^{-1}.

It should be stressed that turnover frequencies depend heavily on the type of experiment (e.g., use of a chemical oxidant or a photogenerated one and, in the latter case, generation by laser flash or continuous irradiation) and, for each type of experiment, on various experimental parameters (oxidant and catalyst concentrations, light intensity). Thus, comparisons between TOF values obtained in different contexts can be misleading. In particular, TOF values obtained by chemical oxidation methods cannot definitely be compared with those obtained in continuous photochemical experiments, where photogeneration of the oxidant is a rate limiting step. The difference between the high values obtained here and the much lower value reported for **1** in continuous photochemical experiments (8.0×10^{-2} s^{-1})[16b] stems clearly from such difference in methods. For the same reasons, comparisons of TOF values obtained by chemical oxidation methods to those exhibited by the oxygen evolving complex of photosystem II, while appealing,[40] should be taken with caution.

CONCLUSIONS

We have examined two main issues relating to the behavior of the tetraruthenium polyoxometalate catalyst **1** in photocatalytic water oxidation cycles: (i) the effects of ion pairing between the catalyst and the $Ru(bpy)_3^{2+}$ sensitizer, and (ii) the kinetics of hole transfer from the oxidized sensitizer to the catalyst.

Electrostatic interaction between the negatively charged catalyst and the positively charged sensitizer in aqueous solution leads to efficient static quenching of the $Ru(bpy)_3^{2+}$ excited state. The quenching takes place in ion-paired species with an average **1**:$Ru(bpy)_3^{2+}$ stoichiometry of 1:4. It occurs by very fast (ca. 2 ps) electron transfer to **1** followed by fast (15−150 ps) charge recombination (reversible oxidative quenching mechanism). This energy wasting process is detrimental to photocatalytic activity, as it competes appreciably with the primary photoreaction of the excited sensitizer with the sacrificial oxidant, even in high ionic strength media. One possibility to minimize ion-pair formation and quenching is to keep the catalyst concentration as low as possible, at the price, however, of slowing down the bimolecular hole-transfer process.

The $Ru(bpy)_3^{3+}$ generated by photoreaction of the excited sensitizer with the sacrificial oxidant $S_2O_8^{2-}$ undergoes bimolecular hole scavenging by catalyst **1** at a remarkably high rate ($3.6 \pm 0.1 \times 10^9$ M^{-1} s^{-1}), emphasizing the kinetic advantages of molecular species over colloidal oxide particles as water oxidation catalysts. It could be remarked that, in sacrificial cycles such as that of Figure 2, the hole-transfer rate is not a major issue,[41] as the main processes potentially competing with hole transfer (recombination between the reduced acceptor and the oxidized sensitizer) are prevented by the irreversible reduction of the sacrificial oxidant. Even in such a case, however, a fast hole scavenging rate is beneficial, as it minimizes the occurrence of self-decomposition of $Ru(bpy)_3^{3+}$,[26] which is the ultimate factor limiting turnover number in these systems.[6a,16c,17a] The issue of the hole-transfer rate will become crucial, on the other hand, for any practical scheme of oxygen generation in nonsacrificial (regenerative) systems, where hole transfer to the catalyst must necessarily compete with some recombination process. The most appealing of such regenerative systems are those in which the oxidized sensitizer is produced by photoinduced electron injection into a nanostructured semiconductor photoanode.[1b,6d,42] In such systems the hole transfer process must efficiently compete with electron−hole recombination.

Besides the first hole scavenging step, monitored with **1** in strong excess relative to $Ru(bpy)_3^{3+}$, flash photolysis can also be used to obtain information on the subsequent steps and final oxygen evolution process involved in the full photocatalytic cycle of Figure 2, by working at much smaller concentrations of **1**. Although the kinetics of the various steps cannot be resolved, flash photolysis at low concentration of **1** gives a clear indication that all these processes are remarkably fast. For instance, in experiments with 0.5 μM **1**, a single molecule of catalyst is shown to undergo as much as 45 turnovers in $Ru(bpy)_3^{3+}$ reduction within 40 ms. Assuming one molecule of oxygen being released after four hole-scavenging events, this implies a very high average TOF (280 s^{-1}) for water oxidation.

ASSOCIATED CONTENT

Supporting Information

EPR spectrum of **1** at pH 7, fitting of kinetic traces and calculation of hole-scavenging bimolecular rate costant, and quenching of the sensitizer emission in 8.0×10^{-2} M phosphate buffer by **1** and by persulfate. This material is available free of charge via the Internet at http://pubs.acs.org.

AUTHOR INFORMATION

Corresponding Author

*E-mail: campagna@unime.it (S.C.), andrea.sartorel (A.S.), snf@unife.it (F.S.).

Notes

The authors declare no competing financial interest.

ACKNOWLEDGMENTS

The authors are grateful to Dr. Claudio Chiorboli for the femtosecond spectrocopy measurememts and to Dr. R. Argazzi for help with the nanosecond transient absorption setup. The authors thank Dr. Marilena Di Valentin and Dr. Enrico Salvadori (Department of Chemical Sciences, University of Padova) for collecting the EPR spectra of **1** at neutral pH. Financial support by the Italian MIUR (PRIN 20085ZXFEE, PRIN 20085M27SS, and FIRB RBAP11C58Y "NanoSolar"), by the University of Padova (PRAT CPDA104105/10), and by Fondazione Cariparo (Nanomode—progetti di eccellenza 2010) is gratefully acknowledged.

REFERENCES

(1) (d) Lewis, N. S.; Nocera, D. G. *Proc. Natl. Acad. Sci. U.S.A.* **2006**, *103*, 15729−15735. (a) Eisenberg, R.; Gray, H. B. *Inorg. Chem.* **2008**,

47, 1697−1699. (b) Herrero, C.; Lassalle-Kaisea, B.; Leibl, W.; Rutherford, A. W.; Aukauloo, A. *Coord. Chem. Rev.* **2008**, *252*, 456−468. (c) Sala, X.; Romero, I.; Rodriguez, M.; Escriche, L.; Llobet, A. *Angew. Chem., Int. Ed.* **2009**, *48*, 2−13. (d) Youngblood, W. J.; Lee, S-H. A.; Maeda, K.; Mallouk, T. E. *Acc. Chem. Res.* **2009**, *42*, 1966−1973.

(2) (a) McEvoy, J. P.; Brudvig, G. W. *Chem. Rev.* **2006**, *106*, 4455−4483. (b) Huynh, M. H. V.; Meyer, T. J. *Chem. Rev.* **2007**, *107*, 5004−5064. (b) Gust, D.; Moore, T. A.; Moore, A. L. *Acc. Chem. Res.* **2009**, *42*, 1890−1898.

(3) See, for example: (a) Lehn, J.-M.; Sauvage, J.-P. *Nouv. J. Chem.* **1977**, *1*, 449−451. (b) Lehn, J.-M.; Sauvage, J.-P.; Ziessel, R. *Nouv. J. Chem.* **1979**, *3*, 423−427. (c) Kiwi, J.; Graetzel, M. *Angew. Chem., Int. Ed. Engl.* **1978**, *17*, 860−861. (d) Harriman, A.; Porter, G.; Walters, P. *J. Chem. Soc., Faraday Trans. 2* **1981**, *77*, 2373−2383.

(4) (a) Jiao, F.; Frei, H. *Energy Environ. Sci.* **2010**, *3*, 1018−1027. (b) Gorlin, Y.; Jamarillo, T. F. *J. Am. Chem. Soc.* **2010**, *132*, 13612−13614.

(5) Harriman, A.; Richoux, M.; Christensen, P. A.; Moseri, S.; Neta, P. *J. Chem. Soc., Faraday Trans. 1* **1987**, *83*, 3001−3014.

(6) (a) Hara, M.; Waraksa, C. C.; Lean, J. T.; Lewis, B. A.; Mallouk, T. E. *J. Phys. Chem. A* **2000**, *104*, 5275−5280. (b) Morris, N. D.; Suzuki, M.; Mallouk, T. E. *J. Phys. Chem. A* **2004**, *108*, 9115−9119. (c) Hoertz, P. G.; Kim, Y. I.; Youngblood, W. J.; Mallouk, T. E. *J. Phys. Chem. B* **2007**, *111*, 6845−6856. (d) Youngblood, W. J.; Lee, S. H. A.; Bobayashi, Y.; Hernandez-Pagan, E. A.; Hoertz, P. G.; Moore, T. A.; Moore, A. L.; Gust, D.; Mallouk, T. E. *J. Am. Chem. Soc.* **2009**, *131*, 926−929.

(7) (a) Kanan, M. W.; Nocera, D. G. *Science* **2008**, *321*, 1072−1075. (b) Surendranath, Y.; Dinca, M.; Nocera, D. G. *J. Am. Chem. Soc.* **2009**, *131*, 2615−2620. (c) Dinca, M.; Surendranath, Y.; Nocera, D. G. *Proc. Natl. Acad. Sci. U.S.A.* **2010**, *107*, 10337−10341.

(8) (a) McDaniel, N. D.; Coughlin, M. J.; Tinker, L. L.; Bernhard, S. *J. Am. Chem. Soc.* **2008**, *130*, 210−217. (b) Ellis, W. C.; McDaniel, N. D.; Bernhard, S.; Collins, T. J. *J. Am. Chem. Soc.* **2010**, *132*, 10990−19991.

(9) (a) Zong, R.; Thummel, R. P. *J. Am. Chem. Soc.* **2005**, *127*, 12802−12803. (b) Concepcion, J. J.; Jurss, J. W.; Templeton, J. L.; Meyer, T. J. *J. Am. Chem. Soc.* **2008**, *130*, 16462−16463. (c) Duan, L.; Xu, Y.; Gorlov, M.; Tong, L.; Andersson, S.; Sun, L. *Chem.—Eur. J.* **2010**, *16*, 4659−4668.

(10) (a) Gersten, S. W.; Samuels, G. J.; Meyer, T. J. *J. Am. Chem. Soc.* **1982**, *104*, 4029−4030. (b) Meyer, T. J.; Huynh, M. H. V.; Thorp, H. H. *Angew. Chem., Int. Ed.* **2007**, *46*, 5284−5304. (c) Liu, F.; Concepcion, J. J.; Jurss, J. W.; Cardolaccia, T.; Templeton, J. L.; Meyer, T. J. *Inorg. Chem.* **2008**, *47*, 1727−1752. (d) Jurss, J. W.; Concepcion, J. J.; Norris, M. R.; Templeton, J. L.; Meyer, T. J. *Inorg. Chem.* **2010**, *49*, 3980−3982.

(11) (a) Deng, Z.; Tseng, H.-W.; Zong, R.; Wang, D.; Thummel, R. P. *Inorg. Chem.* **2008**, *47*, 1835−1848. (b) Xu, Y.; Fischer, A.; Duan, L.; Tong, L.; Gabrielsson, E.; Åkermark, B.; Sun, L. *Angew. Chem., Int. Ed.* **2010**, *49*, 1−5.

(12) (a) Wada, T.; Tsuge, K.; Tanaka, K. *Inorg. Chem.* **2001**, *40*, 329−337. (b) Borzoglian, F.; Mola, J.; Rodriguez, M.; Romero, I.; Nenet-Buchholtz, J.; Fontrodona, X.; Cramer, C. J.; Gagliardi, L.; Llobet, A. *J. Am. Chem. Soc.* **2009**, *131*, 15176−15187. (c) Duan, L.; Xu, Y.; Zhang, P.; Wang, M.; Sun, L. *Inorg. Chem.* **2010**, *49*, 209−215.

(13) (a) Cady, C. W.; Crabtree, R. H.; Brudvig, G. W. *Coord. Chem. Rev.* **2008**, *252*, 444−455. (b) Tagore, R.; Crabtree, R. H.; Brudvig, G. W. *Inorg. Chem.* **2008**, *47*, 1815−1823. (c) Dismukes, G. C.; Brimblecomb, R.; Felton, G. A.; Pryadun, R. S.; Sheats, J. E.; Spiccia, L.; Swiegers, G. F. *Acc. Chem. Res.* **2009**, *42*, 1935−1943. (d) Robinson, D. M.; Go, Y. B.; Greenblatt, M.; Dismukes, C. G. *J. Am. Chem. Soc.* **2010**, *132*, 11467−11469. (e) Brimblecombe, R.; Koo, A.; Dismukes, G. C.; Swiegers, G. F.; Spiccia, L. *J. Am. Chem. Soc.* **2010**, *132*, 2892−2894.

(14) (a) Ferreira, K. N.; Iverson, T. M.; Maghlaoui, K.; Barber, J.; Iwata, S. *Science* **2004**, *303*, 1831−1838. (b) Loll, B.; Kern, J.; Saenger, W.; Zouni, A.; Biesiadka, J. *Nature* **2005**, *438*, 1040−1044. (c) Sproviero, E. M.; Gascon, J. A.; McEvoy, J. P.; Brudvig, G. W.; Batista, V. S. *J. Am. Chem. Soc.* **2008**, *130*, 6728−6730. (d) Umena, Y.; Kawakami, K.; Shen, J. R.; Kamiya, N. *Nature* **2011**, *473*, 55−60.

(15) (a) Sartorel, A.; Carraro, M.; Scorrano, G.; De Zorzi, R.; Geremia, S.; McDaniel, N. D.; Bernhard, S.; Bonchio, M. *J. Am. Chem. Soc.* **2008**, *130*, 5006−5007. (b) Sartorel, A.; Mirò, P.; Salvadori, E.; Romain, S.; Carraro, M.; Scorrano, G.; Di Valentin, M.; Llobet, A.; Bo, C.; Bonchio, M. *J. Am. Chem. Soc.* **2009**, *131*, 16051−16053.

(16) (a) Geletii, Y. V.; Botar, B.; Köegerler, P.; Hillesheim, D. A.; Musaev, D. G.; Hill, C. L. *Angew. Chem., Int. Ed.* **2008**, *47*, 3896−3899. (b) Geletii, Y. V.; Huang, Z.; Hou, Y.; Musaev, D. G.; Lian, T.; Hill, C. L. *J. Am. Chem. Soc.* **2009**, *131*, 7522−7523. (c) Geletii, Y. V.; Besson, C.; Hou, Y.; Yin, Q.; Musaev, D. G.; Quiñonero, D.; Cao, R.; Hardcastle, K. I.; Proust, A.; Kögerler, P.; Hill, C. L. *J. Am. Chem. Soc.* **2009**, *131*, 17360−17370.

(17) (a) La Ganga, G.; Puntoriero, F.; Campagna, S.; Bazzan, I.; Berardi, S.; Bonchio, M.; Sartorel, A.; Natali, M.; Scandola, F. *Faraday Discuss.* **2012**, *155*, 177−190. (b) McCool, N. S.; Robinson, D. M.; Sheats, J. E.; Dismukes, G. C. *J. Am. Chem. Soc.* **2011**, *133*, 11446−11449.

(18) (a) Yin, Q.; Tan, J. M.; Besson, C.; Geletii, Y. V.; Musaev, D. G.; Kuznetsov, A. E.; Luo, Z.; Hardcastle, K. I.; Hill, C. L. *Science* **2010**, *328*, 342−345. (b) Huang, Z.; Luo, Z.; Geletii, Y. V.; Vickers, J. W.; Yin, Q.; Wu, D.; Hou, Y.; Ding, Y.; Song, J.; Musaev, D. G.; Hill, C. L.; Lian, T. *J. Am. Chem. Soc.* **2011**, *133*, 2068−2071.

(19) (a) Dismukes, G. C.; Brimblecombe, R.; Felton, G. A. N.; Pryadun, R. S.; Sheats, J. E.; Spiccia, L.; Swiegers, G. F. *Acc. Chem. Res.* **2009**, *42*, 1935−1943. (b) Brimblecombe, R.; Koo, A.; Dismukes, G. C.; Swiegers, G. F.; Spiccia, L. *J. Am. Chem. Soc.* **2010**, *132*, 2892−2894.

(20) Weakley, T. J. R.; Evans, H. T.; Showell, J. S.; Tourné, G. F.; Tourné, C. M. *J. Chem. Soc., Chem. Commun.* **1973**, 139−140.

(21) (a) Puntoriero, F.; La Ganga, G.; Sartorel, A.; Carraro, M.; Scorrano, G.; Bonchio, M.; Campagna, S. *Chem. Commun.* **2010**, *46*, 4725−4727. (b) Puntoriero, F.; Sartorel, A.; Orlandi, M.; La Ganga, G.; Serroni, S.; Bonchio, M.; Scandola, F.; Campagna, S. *Coord. Chem. Rev.* **2011**, *255*, 2594−2601. (c) Carraro, M.; Sartorel, A.; Toma, F. M.; Puntoriero, F.; Scandola, F.; Campagna, S.; Prato, M.; Bonchio, M. *Top. Curr. Chem.* **2011**, *303*, 120−151.

(22) Stracke, J. J.; Finke, R. G. *J. Am. Chem. Soc.* **2011**, *133*, 14872−14875.

(23) The same behavior, i.e., the molecular metal cluster being not the real catalyst but simply a precursor to the catalytically active metal oxide material, is also exhibited by a related cubane-like manganese cluster,[19,24] and could be a rather general feature for systems involving relative labile metal centers.

(24) Hocking, R. K.; Brimblecombe, R.; Chang, L. Y.; Singh, A.; Cheah, M. H.; Glover, C.; Casey, W. H.; Spiccia, L. *Nat. Chem.* **2011**, *3*, 461−466.

(25) Orlandi, M.; Argazzi, R.; Sartorel, A.; Carraro, M.; Scorrano, G.; Bonchio, M.; Scandola, F. *Chem. Commun.* **2010**, *46*, 3152−3154.

(26) Ghosh, P. K.; Brunschwig, B. S.; Chou, M. H.; Creutz, C.; Sutin, N. *J. Am. Chem. Soc.* **1984**, *106*, 4772−4783.

(27) The strongly oxidizing SO_4^- radical ion undergoes a secondary dark reaction with $Ru(bpy)_3^{2+}$, essentially doubling the quantum yield of P^+ production.[28,29]

(28) Bolletta, F.; Juris, A.; Maestri, M.; Sandrini, D. *Inorg. Chim. Acta* **1980**, *44*, L175−L176.

(29) White, H. S.; Becker, W. G.; Bard, A. J. *J. Phys. Chem.* **1984**, *88*, 1840−1846.

(30) Some preliminary observations on the behavior of **1** were reported in ref 25.

(31) Chiorboli, C.; Rodgers, M. A. J.; Scandola, F. *J. Am. Chem. Soc.* **2003**, *125*, 483−491.

(32) This assignment should be regarded as a tentative. Taking a different assignment of the electrochemical redox steps, as proposed by Hill and co-workers,[16c] the paramagnetic species could be attributed to the III,IV,IV,IV state.

(33) Kalyanasundaram, K. *Photochemistry and Photophysics of Polypyridine and Porphyrin Complexes*; Academic Press: London, 1996.

(34) In the alternative mechanism, the formation of $Ru(bpy)_3^+$ would imply quite different spectral changes, with a sharp positive absorption expected to rise at 500 nm (Creutz, C.; Sutin, N. *J. Am. Chem. Soc.* **1976**, *98*, 6384−6385).
(35) Being obtained under better pseudo-first-order conditions (Figure S3 of Supporting Information), the present value is more precise than the (slightly lower) one reported in a preliminary communication of this work.[25]
(36) A kinetic fit of the delayed component yields a pseudo-first-order rate constant of 5.4×10^5 s^{-1}. With a $Ru(bpy)_3^{2+}$ concentration of 5×10^{-5} M, this corresponds a to bimolecular rate constant of 1.1×10^{10} M^{-1} s^{-1}.
(37) This conclusion can be checked quantitatively by estimating the fraction of free $Ru(bpy)_3^{2+}$ at the various concentrations of **1** by spectrofluorimetry, and knowing the efficiency of the bimolecular quenching with persulfate (Figure S4 of Supporting Information).
(38) This effect, while diminishing the amount of photogenerated $Ru(bpy)_3^{3+}$, is not detrimental from the photocatalytic viewpoint, as it amounts to direct catalyst oxidation, avoiding the intermediate hole-transfer step. The rate of reaction of the SO_4^- radical with **1** can be estimated to be ca. 5 times higher than that with $Ru(bpy)_3^{2+}$ (i.e., ca. 5×10^{10} M^{-1} s^{-1}), considering that an apparent 50% competition between the two pathways takes place when $[\mathbf{1}] = 1 \times 10^{-5}$ M and $[Ru(bpy)_3^{2+}] = 5 \times 10^{-5}$ M.
(39) Using $\Delta\varepsilon = 13\,000$ M^{-1} cm^{-1} and the appropriate correction for the ratio between the volume of solution probed by the analyzing beam and that excited by the laser pulse (1.35, as obtained from saturation techniques).
(40) Duan, L.; Bozoglian, F.; Mandal, S.; Stewart, B.; Privalov, T.; Llobet, A.; Sun, L. *Nat. Chem.* **2012**, *4*, 418−423.
(41) In fact, successful oxygen evolution with the same set of components has been achieved using concentrations of **1** of the order of 10^{-6} M.[16]
(42) With catalyst **1**, extensive sensitizer−catalyst ion pairing is expected to take place at the semiconductor surface, potentially leading to excited state quenching. Fortunately, photoinduced electron injection into the semiconductor from chemically grafted sensitizers is usually extremely fast (mostly in the 10^{-13}−10^{-12} s time scale) so as to prevent, even in an ion-paired situation, quenching by the catalyst. Indeed, in preliminary experiments using a Ru(II) polypyridine complex anchored on TiO_2, on which **1** is electrostatically bound, efficient photoinduced electron injection was observed, followed by hole shift.[25]